

Electronic Structure of Terbium Using the Relativistic Augmented-Plane-Wave Method

C. JACKSON

Solid State Theory Group, Physics Department, Imperial College, London SW7, England

(Received 3 September 1968)

The energy bands for Tb have been calculated by the relativistic augmented-plane-wave method. The resulting Fermi surface is presented, and agreement is found with the characteristic wave vector describing the spiral phase of Tb.

INTRODUCTION

IN recent years, much interest has centered on the study of the ordered magnetic phases of rare-earth metals and a considerable amount of experimental information has been amassed, especially from neutron-scattering measurements.¹ Because of its relatively low neutron-capture cross section and large magnetic moment, a favorable element to study with these techniques is terbium. And, in fact, measurements were made on Tb by Møller *et al.*²

Many of the features of the dynamics of magnetic systems can be related to the Fermi surface. In particular, the interionic indirect exchange interaction in Tb is postulated to be that of Ruderman, Kittel, Kasuya, and Yosida³⁻⁵ (RKKY). This interaction is sensitive to features of the Fermi surface and Roth, Zeiger, and Kaplan⁶ investigated the effect of non-sphericity of the Fermi surface on the RKKY interaction.

As the Fermi surface is derived directly from the energy-band structure, it is then clear that the real energy bands are very important in determining the magnetic ordering. Now some of the magnetic properties may be sensitive to very subtle features of the Fermi surface and so relativistic effects must be taken into account when calculating band structures for the heavy rare earths. The relativistic version of the augmented-plane-wave method (RAPW) is extremely applicable to the rare earths and Keeton and Loucks⁷ applied the RAPW method to a selection of the heavy rare earths.

The RKKY interaction can be related to a wave vector (\mathbf{q}) dependent susceptibility $\chi(\mathbf{q})$ and Evenson and Liu⁸ injected the RAPW heavy rare-earth results of Keeton and Loucks into $\chi(\mathbf{q})$. This gave a simple demonstration of the effects of a realistic band structure. In order to get similar information for Tb, it was

decided to perform an RAPW calculation of its band structure, and this paper presents the results obtained.

PROCEDURE

The crystal structure of terbium is hexagonal close-packed (hcp) with a c/a ratio of 1.58. The crystal potential was calculated using the usual "muffin-tin" approximation, constructed by using the method of Mattheiss.⁹ The muffin-tin radius used was 3.0042 a.u. Exchange effects for the crystal potential were treated by using the Slater $\rho^{1/3}$ approximation.

The free atomic configuration for Tb is $4f^96s^2$ but it is known that the metallic form has three conduction electrons. In order to be able to evaluate the wave functions, which in turn give the charge densities used in constructing the potential, it was decided to use the configuration $4f^96s^2$, although the configuration $4f^85d^16s$ was another possibility. In the paper by Keeton and Loucks⁷ the choice and effects of such configurations is discussed. The wave functions used in RAPW calculations are usually relativistic Hartree-Fock-Slater. However, the wave functions used in this calculation were relativistic Hartree-Fock, in which exchange is treated exactly. These were generated within the group by Coulthard using a computer program developed by him.¹⁰ This gave a more accurate solution for the charge density distribution.

The RAPW method was that proposed by Loucks^{11,12} and this requires solution of the equation

$$\det |M^{ij}(n,m)| = 0,$$

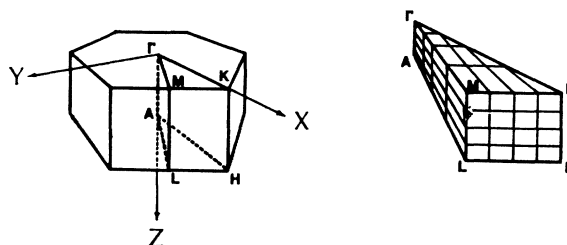


FIG. 1. Lower half of the primitive Brillouin zone for the hcp lattice showing orientation of coordinate axes and $1/24$ zone showing calculation mesh.

¹ W. C. Koehler, H. R. Child, E. O. Wollan, and J. W. Cable, *J. Appl. Phys.* **34**, 1335 (1963).

² H. B. Møller, J. C. G. Houmann, and A. R. Mackintosh, *J. Appl. Phys.* **39**, 807 (1968).

³ M. A. Ruderman and C. Kittel, *Phys. Rev.* **96**, 99 (1954).

⁴ K. Yosida, *Phys. Rev.* **106**, 983 (1959).

⁵ T. Kasuya, *Progr. Theoret. Phys. (Kyoto)* **16**, 45 (1956).

⁶ L. M. Roth, H. J. Zeiger, and T. A. Kaplan, *Phys. Rev.* **149**, 519 (1966).

⁷ S. C. Keeton and T. L. Loucks, *Phys. Rev.* **168**, 672 (1968).

⁸ W. E. Evenson and S. H. Liu, *Phys. Rev. Letters* **21**, 432 (1968).

⁹ L. F. Mattheiss, *Phys. Rev.* **133**, A1399 (1964).

¹⁰ M. A. Coulthard, *Proc. Phys. Soc. (London)* **91**, 44 (1967).

¹¹ T. L. Loucks, *Phys. Rev.* **139**, A1333 (1965).

¹² T. L. Loucks, *Augmented Plane Wave Method* (W. A. Benjamin, Inc., New York, 1966).

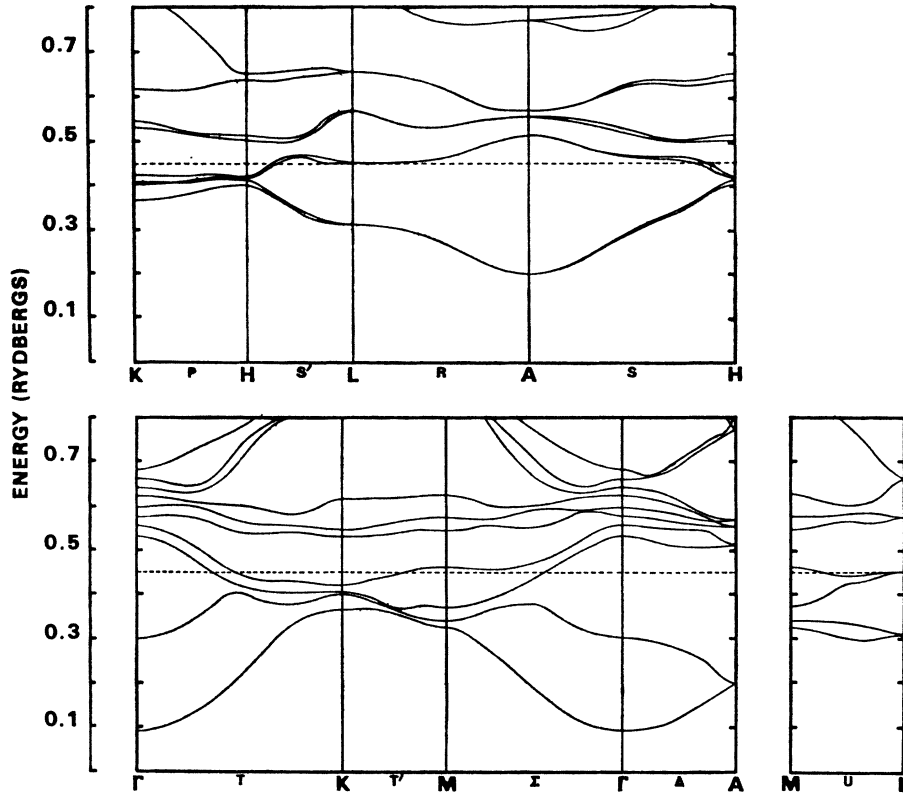


FIG. 2. Energy bands for Tb along symmetry lines. The dashed line is the Fermi level.

where

$$M^{ij}(n,m) = (k_j^2 - E) \left\{ \Omega_0 \delta_{ij} - 4\pi \sum_{\nu} S_{\nu}^2 e^{ik_{ij} \cdot \mathbf{r}_{\nu}} \right. \\ \times \mathcal{G}_1(k_{ij} S_{\nu}) / k_{ij} \delta_{mn} + 4\pi \sum_{\nu} S_{\nu}^2 e^{ik_{ij} \cdot \mathbf{r}_{\nu}} \\ \times \sum_{\kappa} D_{\kappa}^{ij}(n,m) \mathcal{G}_i(k_i S_{\nu}) \mathcal{G}_i(k_j S_{\nu}) (c f_{\kappa}(S_{\nu}) / g_{\kappa}(S_{\nu}) \\ \left. - S_{\kappa} k_j \mathcal{G}_i'(k_j S_{\nu}) / \mathcal{G}_i(k_j S_{\nu}) \right), \\ D_{\kappa}^{ij}(n,m) = 4\pi \sum_{\mu} C(l_{\frac{1}{2}}^j; \mu - n, n) C(l_{\frac{1}{2}}^i; \mu - m, m) \\ \times Y_{l, \mu - n}^*(\hat{k}_j) Y_{l, \mu - m}(\hat{k}_i)$$

and

$$\mathbf{k}_i = \mathbf{k} + \mathbf{G}_i, \quad \mathbf{k}_{ij} = \mathbf{k}_j - \mathbf{k}_i,$$

using the notation of Loucks.¹²

\mathbf{G}_i is the i th reciprocal lattice vector, $\mathcal{G}_l(x)$ are spherical Bessel functions, and $Y_{lm}(x)$ are spherical harmonics. S_{ν} is the radius of the muffin-tin sphere. The C 's are Clebsch-Gordan coefficients, and the prime on \mathcal{G}_l denotes differentiation with respect to $k_j s$ (here evaluated at $s = S_{\nu}$); \mathbf{s} is a position vector originating from the center of the ν th muffin-tin sphere; \mathbf{r}_{ν} is the position vector of the center of the ν th sphere, and Ω_0 is the volume of the unit cell. c is the speed of light and E is the energy eigenvalue at wave vector \mathbf{k} .

The above determinantal equation was solved using 32 reciprocal lattice vectors but for accuracy in de-

termining the Fermi surface this was extended to 40 to give better convergence. The sum over κ was cut off at +9 and -10, i.e., orbital contributions for $l=0$ to 9 were included.

To solve the determinant, values of \mathbf{k} were selected in reciprocal space and the determinant was plotted for different values of E . The zeros of the plot corresponded to the allowed energy eigenvalues. Evaluation of one value of the determinant for a given \mathbf{k} and E was about 15 sec on a PDP-6 computer. The program for 40 reciprocal lattice vectors required 56 000 words of core. The eigenvalues were converged to about 0.005 Ry.

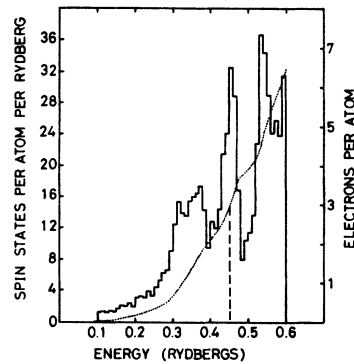


FIG. 3. Density of states for Tb. Dashed line is the Fermi level. Dotted line is the integrated density of states (units for this on the right-hand side).

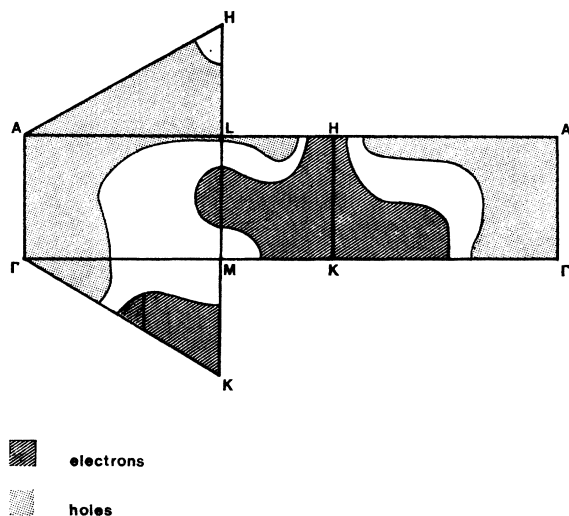


FIG. 4. Intersections of the Fermi Surface with symmetry planes of the Brillouin zone.

The energy eigenvalues were evaluated on a mesh fitted to $1/24$ of the primitive Brillouin zone as in Fig. 1, i.e., for a total of 75 points in reciprocal space.

DENSITY OF STATES

Clearly, in order to be able to construct the density-of-states curve, a larger distribution of points in the Brillouin zone had to be taken. The original mesh of Fig. 1 was close enough to enable the energy eigenvalues at intermediate points to be obtained by a second-order interpolation scheme. The density-of-states results which were evaluated correspond to a sample of 50 226 points in the Brillouin zone.

RESULTS

The energy bands along the symmetry lines of the Brillouin zone are presented in Fig. 2. Directions and points in the zone are labeled using the notation of Herring.¹³ Since band crossings are possible in the Δ , P , S , and S' directions, the connectivity of the bands in these directions, particularly when bands were closely spaced, was slightly uncertain. To remedy this, calculations were performed at closely spaced intervals in the region of an uncertainty of band crossing. A histogram of the density of states is given in Fig. 3. The dotted curve drawn in this figure represents the integrated density of states and the units for this are on the right-hand side. The Fermi energy is at 0.452 Ry. Diagrams showing intersections of the Fermi surface with the symmetry planes are given in Fig. 4. A drawing of the Fermi surface in the reduced zone scheme is presented in Fig. 5. For simplicity of presentation the two parts of the surface, corresponding to band 4 and band 3, are drawn separately.

¹³ C. Herring, J. Franklin Inst. 233, 525 (1942).

DISCUSSION

In discussing these results attention is drawn to two papers; first that of Keeton and Loucks⁷ and secondly that of Møller, Houmann, and Mackintosh.² In the former, the band structure of Dy 2 (i.e., with the free-atom configuration $4f^{10}6s^2$) is presented as typical of the heavy rare earths; while in the latter, the band structure of Tb along the symmetry directions is shown. Particular attention is drawn to the bands between M and L (i.e., in the U direction) in both cases and both these are shown in Fig. 6. In general, bands 3 and 4 become degenerate at L . In Møller's result the degeneracy at L is well below the Fermi level and only band 4 cuts the Fermi level. In the Dy 2 result of Loucks, the degeneracy occurs above the Fermi level and both bands cut the Fermi level. The similarity here between our result and that of Loucks is clear, and in our result, the degeneracy at L occurs just above the Fermi level. As these bands are flat and are very near the Fermi level, the Fermi surface they produce could be very sensitive to changes in the potential. However, the purpose of these calculations is to look for general features and trends and our result certainly agrees very well with the other rare-earth results of Keeton and Loucks. The discrepancy between Møller's band struc-

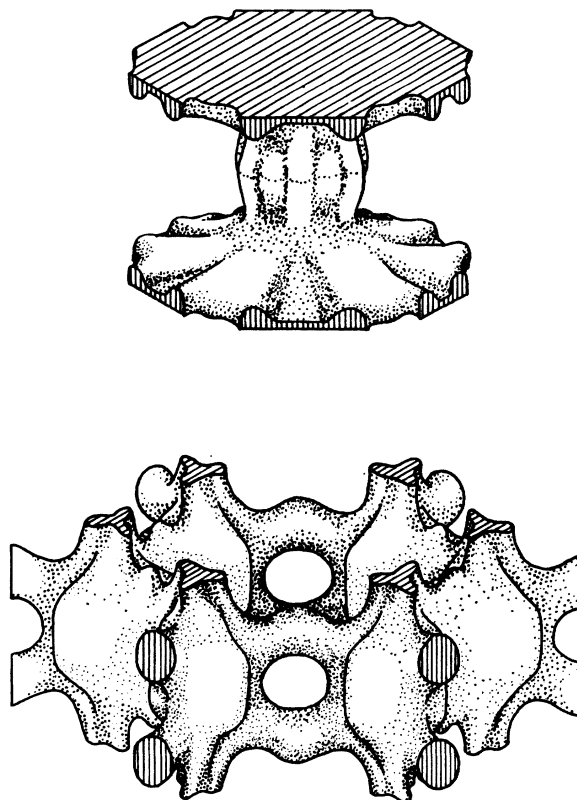


FIG. 5. The Fermi surface of Tb drawn in the reduced zone scheme. The central column of holes and the electron pipework are drawn separately. The latter surface is shown extending into other equivalent zones.

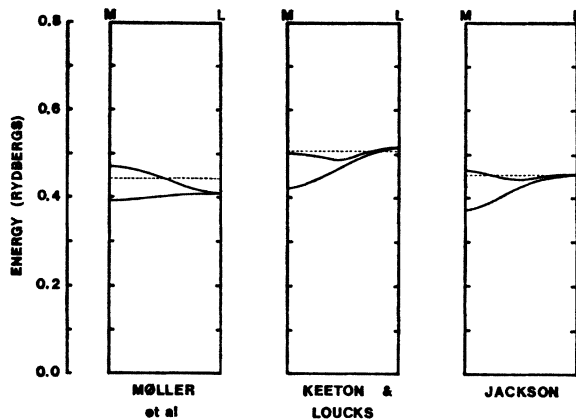


FIG. 6. Energy bands 3 and 4 between M and L (U direction) as evaluated by Möller *et al.*, Keeton and Loucks, and the present work.

ture and the other results is due to their use of an incorrect potential.¹⁴

As spin-orbit coupling effects are included in the RAPW method then the degeneracy which would exist over all of the ALH plane is lifted and, except along the AL line, spin-orbit coupling reduces all four-fold degeneracies to pairs of doubly degenerate states.¹⁵ Thus there is hardly any point in presenting drawings of the Fermi surface in the double zone scheme as we would have discontinuities in surface over the ALH plane. The Fermi surface in the reduced zone scheme consists of two surfaces. An "Ionic column" of holes due to band 3, and, surrounding this, a collection of bottles and pipes of electrons due to band 4. The features of the Fermi surface which are most sensitive (due to bands 3 and 4 becoming degenerate at L) to the value of the Fermi energy are those near L , i.e., those pieces of horizontal pipe near the ALH surface and to a greater extent that part of the ionic column's capital where it rises up to L .

A useful check on this calculation is to examine the consequences of the theory of Williams, Loucks, and Mackintosh¹⁶ on the Q vector characterizing the periodic magnetically ordered phases of the rare earths. This theory was modified by Keeton and Loucks⁷ when they

¹⁴ A. R. Mackintosh (private communication).

¹⁵ L. F. Mattheiss, *Phys. Rev.* **151**, 450 (1966).

¹⁶ R. W. Williams, T. L. Loucks, and A. R. Mackintosh, *Phys. Rev. Letters* **16**, 168 (1966).

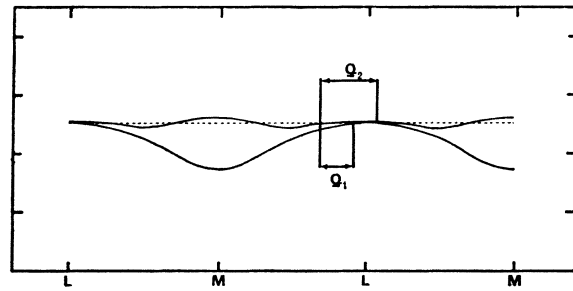


FIG. 7. Energy bands 3 and 4 in the U direction displayed in two zones.

correctly point out that the Q vector between electron and hole parallel sheets in the reduced zone scheme is not important. Referring to Fig. 7, this would be the vector Q_1 . What is important is the coupling between regions of parallel Fermi surface where the slopes of bands producing this surface are of opposite sign. Coupling between these states gives a very much more favorable situation energetically, and the characteristic Q vector is Q_2 as shown. The vector Q_2 may be alternatively displayed in the double zone scheme.⁷ From our result the characteristic Q due to the flat portion of the hole column's capital and the electron pipework nesting in the manner of Q_2 is $0.29\pi/c$. The experimentally determined Q of the spiral phase is $0.224\pi/c$.¹⁷ When this result is placed in the table constructed by Keeton and Loucks for the rare earths Y, Lu, Er, Dy, and Gd, the agreement with their theory and with experiment is quite remarkable. A transformation of our Fermi surface into their double zone scheme also shows their prediction of the "webbing" feature to be remarkably accurate.

ACKNOWLEDGMENTS

The author wishes to thank Dr. R. L. Jacobs and Professor E. P. Wohlfarth for numerous discussions, and Professor C. C. Butler for the use of a considerable amount of computer time. The author is also grateful for the patience of the artist M. E. Thomas in drawing the Fermi surface. Finally, the author wishes to thank the Science Research Council for financial support while this work was carried out.

¹⁷ K. Yosida and A. Watabe, *Progr. Theoret. Phys. (Kyoto)* **28**, 361 (1962).

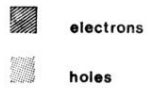
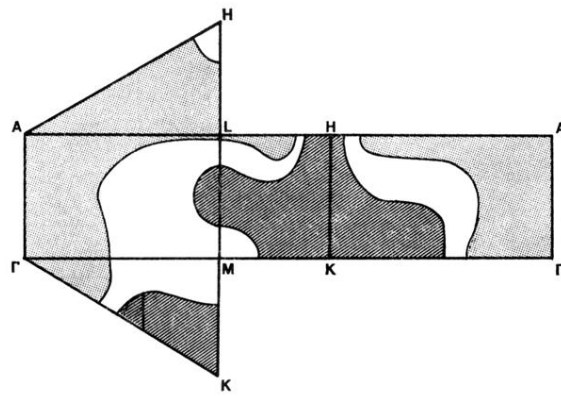


FIG. 4. Intersections of the Fermi Surface with symmetry planes of the Brillouin zone.